

Energy-based Modelling and Simulation of a Series Hybrid Electric Vehicle Propulsion System

Raúl S. Muñoz-Aguilar*, Arnau Dòria-Cerezo* and Paul F. Puleston**

*Department of Electrical Engineering and Institute of Industrial and Control Engineering,
Universitat Politècnica de Catalunya, Spain

{raul.munoz-aguilar, arnau.doria}@upc.edu

**CONICET and the LEICI, Faculty of Engineering,
National University of La Plata, 1900 La Plata, Argentina

puleston@ing.unlp.edu.ar

Acknowledgments

A. Dòria-Cerezo was partially supported by the Spanish government research project DPI2007-62582.

Keywords

<<Hybrid Electric Vehicle>>, <<Modelling>>, <<AC Machine>> .

Abstract

This paper presents an energy-based model of a series hybrid electric vehicle. The proposed propulsion system has a new configuration using a wound-rotor synchronous generator (WRSM) and a doubly-fed induction machine (DFIM). From the classic dq dynamical equations of the WRSM and DFIM the port-controlled Hamiltonian models of each machine is described. One of the abilities of the port-based models is that the complete model is easy to obtain by means of interconnection rules. Following this, the Hamiltonian model of the whole system is obtained. Similarly, the bond graph approach allows to build a complex model by interconnecting several subsystems. This paper also contains bond graph models of the machines and the propulsion system. Numerical simulations are also presented in order to validate the proposed models.

Introduction

Hybrid electrical vehicles (HEV) are the focus of many research interests because they are able to provide good performance and long operating time [1]. Basically, the HEV is composed of an internal combustion engine, an electrical machine and a battery pack. The main goal of this structure is to reduce the CO_2 emissions by means of the regenerative braking using the electrical machine, both as a motor drive or as a generator, which charges or discharges the batteries. It is also desired to keep the drivability performance of the vehicle [2]. Depending on the topology, HEV can be divided into two basic configurations: parallel and series.

In this work we focus on the advanced topologies of series HEV. The use of wound-rotor machines (as doubly-fed induction machines) has been studied in [3] and [4]. These systems had some performance limitations because they are unable to control intermediate variables between both machines. More control inputs are necessary in order to achieve a good control for HEV purposes. The propulsion system we propose consists of a wound-rotor synchronous generator (WRSM) and a doubly-fed induction machine (DFIM). The main advantage of this system is the ability to manage the energy without a power converter between both machines. In this case the power management is done through the rotor voltages of the DFIM and the field voltage of the WRSM.

Energy-based modelling describes dynamical systems from a physical point of view, representing the power flowing between the different elements, where the energy is stored and dissipated. Generally, these techniques are based on the network modelling and the port interconnection between several subsystems. One implementation of this idea is known as port Hamiltonian systems or port-controlled Hamiltonian systems (PCHS) [5][6]. One of the interest of this description is that the obtained models facilitate

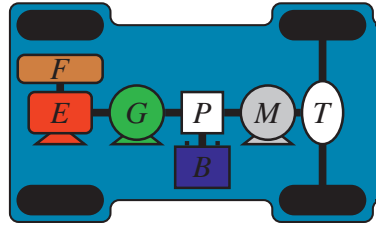


Figure 1: Series HEV scheme.

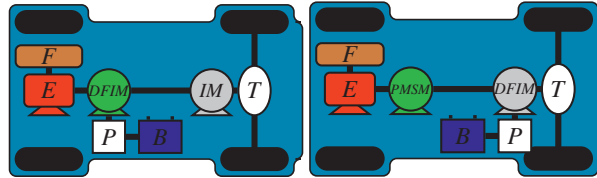


Figure 2: Advanced series HEV topologies.

the design of non-linear controllers using passivity-based techniques, such as the interconnection and damping assignment (IDA-PBC) method [7].

PCHS theory provides the mathematical foundation of the bond graph approach, which allows to model dynamical systems graphically, describing the energy flowing through different elements, which represents source, storage, dissipative and transmission elements [8]. The bond graph description permits the integration of submodels easily and, by means of a simple computer algorithm, the simulation-ready equations of a complex model can be derived.

In this work we present the port-controlled Hamiltonian and bond graph descriptions of a new series HEV topology.

System description

Fig. 1 shows the classic configuration of a series HEV [2]. It contains an internal combustion engine (ICE), two electrical machines connected by a power converter which also is connected to the batteries. Series HEV offers several advantages; the ICE is mechanically decoupled from the transmission, the final torque is given by an electrical machine (which have a near-ideal torque speed characteristics) and also simple management strategies can be adopted [1]. One of the disadvantages of this topology is that all the power flows through the power converter and, consequently, the losses are high.

Wound-rotor electrical machines offer the main advantage that the rotor voltages can be used for control purposes. Based on this, previous works proposed DFIM [3][4] as electrical machines for HEV applications (see Fig. 2). The feature of this kind of topologies is that the power converter could be eliminated from the stator and, consequently, losses can be reduced. The so-called Joint System [3] used a DFIM as generator, with an induction machine as a motor. In [4], the Variable Voltage Variable Frequency scheme was introduced, with the DFIM as a motor with a permanent magnet synchronous machine (PMSM) for the generating part.

But the topologies presented in [3] and [4] are not able to control efficiently the system reactive power and stator voltage amplitudes simultaneously. To overcome this drawback, a new topology for a series HEV is introduced in this paper.

Figure 3 shows the electrical connection of a new series HEV topology. The WRSM is mechanically connected with the ICE, and operates as a generator. The WRSM and DFIM stator sides are directly connected while the mechanical port of the DFIM is coupled to the HEV transmission. Notice that the DFIM acts either in generator or motor mode. Both machines (WRSM and DFIM) are rotor connected to the batteries by means of DC/DC and AC/DC converters, respectively.

This new scheme defines four control inputs: the field (or rotor) voltage of the WRSM, v_F , the two rotor dq -voltage components of the DFIM, $v_r \in \mathbb{R}^2$, and the mechanical torque produced by the ICE¹, τ_W . These four control variables are able to control the electrical torque produced by the DFIM, to manage the power flow and to keep a stator voltage to its nominal value together with a stator power factor close to one.

¹In this paper, the ICE is considered as an ideal torque source.

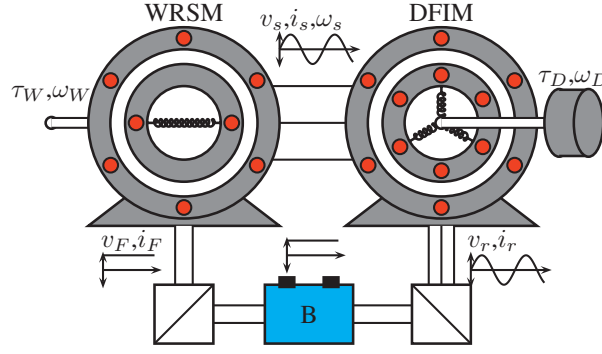


Figure 3: Electrical scheme of the proposed propulsion system.

In this work only the energy-based modelling is presented. The development of robust and highly efficient energy management policies and control laws will be considered in future work.

Port controlled Hamiltonian model

Hamiltonian modelling uses state dependent energy functions to characterize the dynamics of the different subsystems, and connects them using a Dirac structure, which embodies the power preserving network of relationships established by the corresponding physical laws. The result is a mathematical model with an specific structure, called port-controlled Hamiltonian system (PCHS) [6], which lends itself to a natural, physics-based analysis and control design.

Port-controlled Hamiltonian systems can be seen as a mathematical description of the bond graphs [9]. An explicit PCHS has the form [5]

$$\begin{cases} \dot{x} &= (j(x) - \mathcal{R}(x))\partial H + g(x)u \\ y &= g^T(x)\partial H \end{cases} \quad (1)$$

where $x \in \mathbb{R}^n$ are the energy variables (or state vector), $u, y \in \mathbb{R}^m$ are the port variables, and $H(x) : \mathbb{R}^n \rightarrow \mathbb{R}$ is the Hamiltonian function, representing the energy function of the system. The ∂_x (or ∂ , if no confusion arises) operator defines the gradient of a function of x and, in the sequel, we will take it as a column vector. $j(x) \in \mathbb{R}^{n \times n}$ is the interconnection matrix, which is skew-symmetric ($j(x) = -j(x)^T$), representing the internal energy flow in the system, and $\mathcal{R}(x) \in \mathbb{R}^{n \times n}$ is the dissipation matrix, symmetric and, in physical systems, positive semidefinite ($\mathcal{R}(x) = \mathcal{R}(x)^T \geq 0$), which accounts for the internal losses of the system. Finally, $g(x) \in \mathbb{R}^{n \times m}$ is an interconnection matrix describing the port connection of the system to the outside world. It yields the flow of energy to/from the system through the port variables, u and y , which are conjugated, *i.e.* their dot product has units of power.

Usually, three-phase electrical machine modelling uses the so-called Park (or dq) transformation. This mathematical transformation allows to decouple variables and to facilitate the solution of difficult equations which depends on the rotor position [10]. With the dq transformation the abc three-phase variables (voltages and currents) are reduced to a two-phase dq variables. The reference frame for the Park transformation depends on the application.

In this case, the selected reference is the mechanical angle of the WRSM. Note that in such synchronous machine, the mechanical speed (ω_W) matches the stator frequency (ω_s) (assuming one pair of poles).

In this section, from the standard dq models of the DFIM and WRSM, the PCHS are derived and the whole interconnected Hamiltonian system is also obtained. Machines of one pair of poles are considered.

PCHS of a doubly-fed induction machine

The PCHS of a doubly-fed induction machine has been presented in [11]. The Hamiltonian variables are

$$x_D^T = [\lambda_D^T, p_D] = [\lambda_{sD}^T, \lambda_r^T, p_D] \in \mathbb{R}^5$$

where $\lambda_{sD} = [\lambda_{sDd}, \lambda_{sDq}]^T$ and $\lambda_r = [\lambda_{rd}, \lambda_{rq}]^T$ are the stator and rotor fluxes in dq -coordinates, respectively, $p_D = J_D \omega_D$ is the mechanical momentum, ω_D is the mechanical speed and J_D is the inertia of the rotating parts. Note that the D subindex has been included to refer to the DFIM.

The interconnection and damping matrices are, respectively,

$$J_D = \begin{bmatrix} -\omega_s L_{sD} J_2 & -\omega_s L_{sr} J_2 & O_{2 \times 1} \\ -\omega_s L_{sr} J_2 & -(\omega_s - \omega_D) L_r J_2 & L_{sr} J_2 i_{sD} \\ O_{1 \times 2} & L_{sr} i_{sD}^T J_2 & 0 \end{bmatrix} \in \mathbb{R}^{5 \times 5}$$

$$R_D = \begin{bmatrix} R_{sD} I_2 & O_{2 \times 2} & O_{2 \times 1} \\ O_{2 \times 2} & R_r I_2 & O_{2 \times 1} \\ O_{1 \times 2} & O_{1 \times 2} & B_D \end{bmatrix} \in \mathbb{R}^{5 \times 5}$$

where $i_{sD}, i_r \in \mathbb{R}^2$ are the stator and rotor currents, R and L are resistance and inductances², ω_s is the stator electric frequency, B_D is the mechanical damping,

$$J_2 = \begin{bmatrix} 0 & -1 \\ 1 & 0 \end{bmatrix}, \quad I_2 = \begin{bmatrix} 1 & 0 \\ 0 & 1 \end{bmatrix}$$

and $O_{* \times *}$ represents zero matrices.

Fluxes, λ_D , and currents, $i_D^T = [i_{sD}^T, i_r^T] \in \mathbb{R}^4$, are related by

$$\lambda_D = \mathcal{L}_D i_D \tag{2}$$

where the inductance matrix, \mathcal{L}_D , is

$$\mathcal{L}_D = \begin{bmatrix} L_{sD} I_2 & L_{sr} I_2 \\ L_{sr} I_2 & L_r I_2 \end{bmatrix} \in \mathbb{R}^{4 \times 4}.$$

The port connection is represented by

$$g_D = \begin{bmatrix} I_2 & O_{2 \times 2} & O_{2 \times 1} \\ O_{2 \times 2} & I_2 & O_{2 \times 1} \\ O_{1 \times 2} & O_{1 \times 2} & 1 \end{bmatrix} \in \mathbb{R}^{5 \times 5}.$$

with the port variables $u_D^T = [v_{sD}^T, v_r^T, \tau_D]$, where $v_{sD}, v_r \in \mathbb{R}^2$ are the stator and rotor voltages and τ_D is an external torque. The Hamiltonian model is completed with the energy function

$$H_D(x_D) = \frac{1}{2} \lambda_D^T \mathcal{L}_D^{-1} \lambda_D + \frac{1}{2J_D} p_D^2.$$

PCHS of a wound-rotor synchronous machine

A Port-controlled Hamiltonian model of a synchronous machine, with permanent magnet, can be found in [12]. The wound rotor synchronous machine includes a rotor winding which has to be considered. In this case, the Hamiltonian variables are

$$x_W^T = [\lambda_W^T, p_W] = [\lambda_{sW}^T, \lambda_F, p_W] \in \mathbb{R}^4$$

where $\lambda_{sW} = [\lambda_{sWd}, \lambda_{sWq}]^T$ is the stator inductor flux in dq -coordinates, λ_F is the rotor (or field) inductor flux, $p_W = J_W \omega_W$ is the mechanical momentum, ω_W is the mechanical speed, and J_W is the inertia of the rotating parts. The W subindex has been included to refer to the WRSM.

The interconnection and damping matrices are, respectively,

$$J_W = \begin{bmatrix} -\omega_W L_{sW} J_2 & O_{2 \times 1} & -M i_F \\ O_{1 \times 2} & 0 & 0 \\ M^T i_F & 0 & 0 \end{bmatrix} \in \mathbb{R}^{4 \times 4}$$

²Subindexes s and r refers to stator and rotor respectively.

$$\mathcal{R}_W = \begin{bmatrix} R_{sW}I_2 & O_{2 \times 1} & O_{2 \times 1} \\ O_{1 \times 2} & R_F & 0 \\ O_{1 \times 2} & 0 & B_W \end{bmatrix} \in \mathbb{R}^{4 \times 4}$$

where $i_{sW} \in \mathbb{R}^2$ are the stator currents, i_F is the rotor (or field) current, R and L are resistance and inductances³, B_W is the mechanical damping and

$$M = \begin{bmatrix} 0 \\ L_m \end{bmatrix} \in \mathbb{R}^{2 \times 1},$$

with L_m being the mutual inductance.

The WRSM fluxes, λ_W , and currents, $i_W^T = [i_{sW}^T, i_F] \in \mathbb{R}^3$, are related by

$$\lambda_W = \mathcal{L}_W i_W \quad (3)$$

and the inductance matrix, \mathcal{L}_W , is

$$\mathcal{L}_W = \begin{bmatrix} L_{sW}I_2 & M \\ M^T & L_F \end{bmatrix} \in \mathbb{R}^{3 \times 3}.$$

The port connection, g_W , is represented by an identity 4×4 matrix,

$$g_W = I_4,$$

with the port variables $u_W^T = [v_{sW}^T, v_F, \tau_W]$, where $v_{sW} \in \mathbb{R}^2$ is the stator voltages, v_F is the rotor (or field) voltage, and τ_W is the applied external torque. Finally, the Hamiltonian function is

$$H_W(x_W) = \frac{1}{2} \lambda_W^T \mathcal{L}_W^{-1} \lambda_W + \frac{1}{2J_W} p_W^2.$$

PCHS of the whole system

As it is shown in Figure 3 both machines are interconnected through their stator windings. This implies that

$$v_{sD} = v_{sW} = v_s \quad (4)$$

$$i_{sD} = -i_{sW} = i_s \quad (5)$$

$$\omega_s = \omega_W.$$

This particular way of interconnecting the electric machines implies the series connection of two inductors, therefore we define a new variable, $\lambda_s \in \mathbb{R}^2$, such that

$$\lambda_s = \lambda_{sD} - \lambda_{sW}, \quad (6)$$

Using (2) and (3), (6) it can be written as

$$\lambda_s = (L_{sD} + L_{sW})I_2 i_s + L_{sr}I_2 + M i_F, \quad (7)$$

or, differentiating,

$$\dot{\lambda}_s = \dot{\lambda}_{sD} - \dot{\lambda}_{sW}. \quad (8)$$

Notice that defining the new state variable as

$$x^T = [\lambda_s^T, \lambda_r^T, \lambda_F, p_D, p_W] \in \mathbb{R}^7$$

and with (7) and (8), a new Hamiltonian system (1) can be obtained with a Hamiltonian function

$$H(x) = \frac{1}{2} \lambda^T \mathcal{L}^{-1} \lambda + \frac{1}{2J_D} p_D^2 + \frac{1}{2J_W} p_W^2$$

³Subindexes s and F refers to stator and field respectively.

where fluxes $\lambda^T = [\lambda_s^T, \lambda_r^T, \lambda_F] \in \mathbb{R}^5$ and currents $i^T = [i_s^T, i_r^T, i_F] \in \mathbb{R}^5$ are related by, $\lambda = \mathcal{L} i$, with a new inductance matrix, \mathcal{L}

$$\mathcal{L} = \begin{bmatrix} (L_{sD} + L_{sW})I_2 & L_{sr}I_2 & M \\ L_{sr}I_2 & L_r I_2 & O_{2 \times 1} \\ M^T & O_{1 \times 2} & L_F \end{bmatrix}.$$

The interconnection and dissipation matrices are now,

$$j = \begin{bmatrix} -\omega_W(L_{sD} + L_{sW})J_2 & -\omega_W L_{sr}J_2 & O_{2 \times 1} & O_{2 \times 1} & -Mi_F \\ -\omega_W L_{sr}J_2 & -(\omega_W - \omega_D)L_r J_2 & O_{2 \times 1} & L_{sr}J_2 i_s & O_{2 \times 1} \\ O_{1 \times 2} & O_{1 \times 2} & 0 & 0 & 0 \\ O_{1 \times 2} & L_{sr} i_s^T J_2 & 0 & 0 & 0 \\ M^T i_F & O_{1 \times 2} & 0 & 0 & 0 \end{bmatrix}$$

$$\mathcal{R} = \begin{bmatrix} (R_{sD} + R_{sW})I_2 & O_{2 \times 2} & O_{2 \times 1} & O_{2 \times 1} & O_{2 \times 1} \\ O_{2 \times 2} & R_r I_2 & O_{2 \times 1} & O_{2 \times 1} & O_{2 \times 1} \\ O_{1 \times 2} & O_{1 \times 2} & R_F & 0 & 0 \\ O_{1 \times 2} & O_{1 \times 2} & 0 & B_D & 0 \\ O_{1 \times 2} & O_{1 \times 2} & 0 & 0 & B_W \end{bmatrix}$$

and

$$g = \begin{bmatrix} O_{2 \times 2} & O_{2 \times 1} & O_{2 \times 1} & O_{2 \times 1} \\ I_2 & O_{2 \times 1} & O_{2 \times 1} & O_{2 \times 1} \\ O_{1 \times 2} & 1 & 0 & 0 \\ O_{1 \times 2} & 0 & 1 & 0 \\ O_{1 \times 2} & 0 & 0 & 1 \end{bmatrix}$$

with the input variables $u^T = [v_r^T, v_F, \tau_D, \tau_W] \in \mathbb{R}^5$.

Bond graph model

Bond graph theory is a powerful technique to model physical systems [8]. This approach is based on the power flow between the different elements of the system. In other words, bond graph can be seen as a graphical representation of the Port-controlled Hamiltonian systems. The choice of bond graph allows to describe the systems keeping the information of energy generation, storage, dissipation, and transfer, which can help to eventually design both, low-level and supervisory control algorithms.

Many electrical machines are described using the bond graph approach. From the DC machine [8] or AC generator [13], to three-phase induction machines [14][15]. HEV are also modelled using this graphic tool. In [16] a complete bond graph model for a long urban transit bus is obtained and simulated. A bond graph model of a parallel HEV system is presented in [17]. In that case, the electrical machine and internal combustion engine were modelled as an ideal torque sources (Se-element), while the main contribution was focused in the transmission, aerodynamics and wheel models.

The bond graph model of the electrical machines are obtained from the dynamical equations presented. The bond graph model of a doubly-fed induction machine and the wound-rotor synchronous machines are depicted in figures 4 and 5, respectively. For this modelling the l-elements L_{lsD} , L_{lr} , L_{lsW} , L_{lF} are defined as

$$\begin{aligned} L_{lsD} &= L_{sD} - L_{sr} \\ L_{lr} &= L_r - L_{sr} \\ L_{lsW} &= L_{sW} - L_m \\ L_{lF} &= L_F - L_m. \end{aligned}$$

Notice that, from the WRSM model, the bond graph of a permanent magnet synchronous machine (PMSM) can be easily obtained by replacing the field dynamics by a constant flux, ϕ . It implies to eliminate all elements around the up-right 1-junction, and then the MGY becomes a standard GY-element, with a ϕ -depending gyrator modulus.

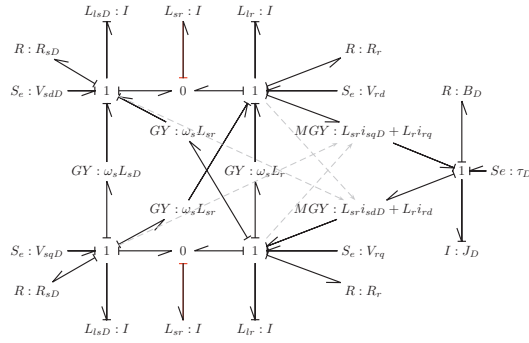


Figure 4: Bond graph model of a doubly-fed induction machine.

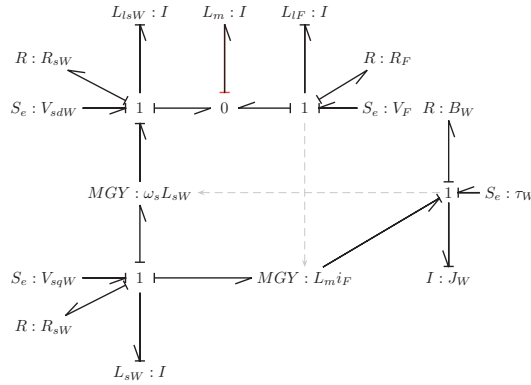


Figure 5: Bond graph model of a wound-rotor synchronous machine.

The whole model can be obtained interconnecting the WRSM and the DFIM through the stator side of both machines. The interconnection rules are described in the previous section, which corresponds to equations (4) and (5).

Finally, the bond graph scheme for the complete model is shown in Fig. 6. Notice that, besides the differential causality assignments internal to the two machines (L_{sr} and L_m), there are extra ones (one for each dq coordinate) due to the way the machines are connected, (see the L_{lsD} elements).

Simulation results

In this Section numerical simulations are presented in order to validate the obtained models. The WRSM was controlled via a PI controller. The DFIM uses a nested control system. An outer PI controller generates the speed reference for an inner current controller, designed accordingly to [14]. Simulations were performed using the 20sim software which contains a bond graph editor.

The DFIM (37kW) and WRSM (37.5kW) parameters are, respectively: $R_{sD} = 0.08233\Omega$, $R_r = 0.0503\Omega$, $L_s = 27.834\text{mH}$, $L_r = 27.834\text{mH}$, $L_{sr} = 27.11\text{mH}$, $J_D = 0.37\text{Kgm}^2$, $B_D = 0.02791\text{Nmrad}^{-1}\text{s}^{-1}$, and $L_{sW} = 26.25\text{mH}$, $R_{sW} = 0.181\Omega$, $L_m = 25.29\text{mH}$, $L_f = 27.19\text{mH}$, $R_f = 0.1002\Omega$ and the WRSM me-

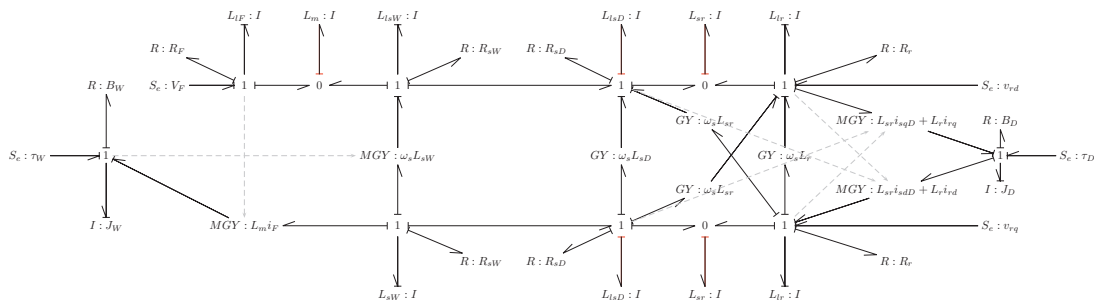


Figure 6: Bond graph model of the complete system.

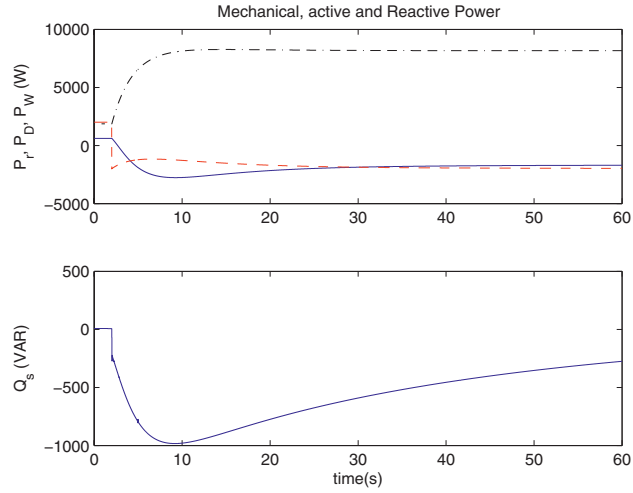


Figure 7: Simulation results: WRSM mechanical power (P_W , dashed-dotted black line), DFIM mechanical power (P_D , dashed red line), rotor active power (P_r , continuous blue line), and stator reactive power (Q_s , below).

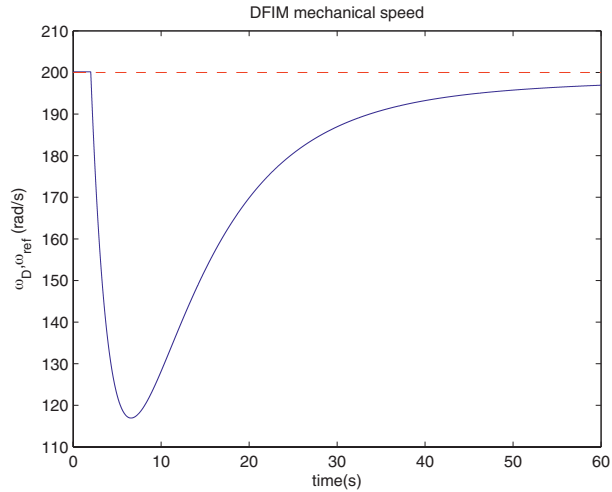


Figure 8: Simulation results: DFIM mechanical speed and its reference.

mechanical speed is fixed at $\omega = 314 \text{ rad s}^{-1}$. The machines rated power are: $P_W = 37.5 \text{ kVA}$ and $P_D = 37 \text{ kVA}$. The controllers parameters are for the WRSM: $K_p = 30$, $K_i = 3$; for the DFIM inner current loop: $K_p = 0.4$, $K_i = 0.009$, for the outer loop: $K_p = 0.1$, $K_i = 0.01$.

The control objectives are: regulate the stator voltage ($V = 400 \text{ V}$), regulate the DFIM mechanical speed ($\omega_r = 200$) and zeroing the stator reactive power ($Q_s = 0$).

The DFIM load torques starts at $\tau_D = 10 \text{ Nm}$ and changes to $\tau_D = -10 \text{ Nm}$ at $t = 2 \text{ s}$. With this values two modes can be observed. Firstly, the system is storing energy into the batteries. Secondly, power is provided by the batteries.

Figure 7 shows the mechanical power flow (computed from $P = \tau\omega$), the rotor active power, P_r , and the stator reactive power⁴, Q_s . As explained before, the rotor active power changes is bidirectional and allows to store energy into the batteries.

Figure 8 shows the DFIM mechanical speed and its reference. Figure 9 shows the rotor amplitude, the stator amplitude and the field voltage, respectively.

⁴In the dq coordinates, the instantaneous active and reactive power can be computed as $P_r = v_r^T i_r$ and $Q_s = v_s^T J_2 i_s$.

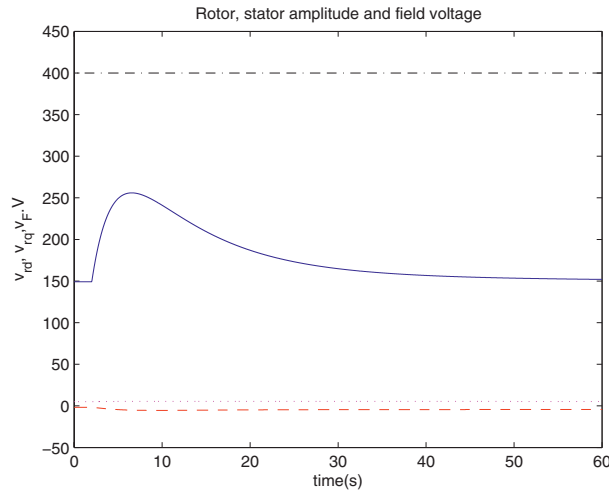


Figure 9: Simulation results: Rotor (v_{rd} , continuous blue line, v_{rq} , dashed red line), stator amplitude (V , dashed-dotted black line) and field voltage (v_F , dotted magenta line).

Conclusions

An alternative architecture for a series HEV propulsion system has been proposed, analysed and modelled. The complex system under study has been divided into several subsystems, described in the electrical and mechanical domains. Two energy-based models were presented, following the Hamiltonian formalism and the bond graph approach.

The proposed models of the novel series HEV topology has been comprehensively assessed through simulations, showing satisfactory results. As additional feature, the submodel integration capability, inherent to bond graph technique, allows to easily expand the proposed model, by interconnection with other mechanical (transmission, wheels, aerodynamics...) and electrical parts (power converters, batteries,...), in future works. Moreover, from a control viewpoint, the presented PCH model will be of great help to design passivity-based controllers.

References

- [1] M. Ehsani, Y. Gao, S.E. Gay, and A. Emadi. *Modern Electric, Hybrid Electric, and Fuel Cell Vehicles: Fundamentals, Theory, and Design*. CRC, Boca Raton, FL, 2004.
- [2] J.M. Miller. *Propulsion systems for hybrid vehicles*. IEE, Power and Energy series, 2004.
- [3] P. Caratozzolo, E. Fossas, J. Pedra, and J. Riera. Dynamic modeling of an isolated motion system with dfig. In *Proc. of the VII IEEE International Power Electronics Congress*, pages 287–292, 2000.
- [4] T. Ortmeier. Variable voltage variable frequency options for series hybrid vehicles. In *Proc. of IEEE Conference on Vehicle Power and Propulsion*, pages 262–267, 2005.
- [5] M. Dalsmo and A. van der Schaft. On representations and integrability of mathematical structures in energy-conserving physical systems. *SIAM J. Control Optim.*, 37:54–91, 1998.
- [6] A. van der Schaft. *L₂ gain and passivity techniques in nonlinear control*. Springer, 2000.
- [7] R. Ortega, A. van der Schaft, B. Maschke, and G. Escobar. Interconnection and damping assignment passivity-based control of port-controlled Hamiltonian systems. *Automatica*, 38(4):585–596, 2002.
- [8] D. Karnopp, D. Margolis, and R. Rosenberg. *System Dynamics: Modeling and Simulation of Mechatronic Systems*. John Wiley and Sons, Inc, 2006.
- [9] G. Golo, A.J. van der Schaft, P.C. Breedveld, and B. Maschke. Hamiltonian formulation of Bond Graphs. In *Workshop NACO II*, pages 2642–2647, 2001.
- [10] P. Krause, O. Wasynczuk, and S. Sudhoff. *Analysis of Electric Machinery and Drive Systems*. John-Wiley and Sons, 2002.

- [11] C. Batlle, A. Dòria-Cerezo, and R. Ortega. Power Flow Control of a Doubly-Fed Induction Machine Coupled to a Flywheel. *European Journal of Control*, 11(3):209–221, 2005.
- [12] Y. Guo, Z. Xi, and D. Cheng. Speed regulation of permanent magnet synchronous motor via feedback dissipative hamiltonian realisation. *IET Control Theory Appl.*, 1(1):281–290, 2007.
- [13] C. Batlle and A. Dòria-Cerezo. Bond graph models of electromechanical systems. the ac generator case. In *IEEE Int. Symp. on Industrial Electronics*, 2008.
- [14] C. Batlle and A. Dòria-Cerezo. Energy-based modeling and simulation of the interconnection of a back-to-back converter and a doubly-fed induction machine. In *American Control Conference*, pages 1851–1856, 2006.
- [15] J. Kim and M. Bryant. Bond graph model of a squirrel cage induction motor with direct physical correspondence. *Journal of Dynamic Systems, Measurement and Control*, 22:461–469, 2000.
- [16] G. Hubbard and K. Youcef-Toumi. Modeling and simulation of a hybrid-electric vehicle drivetrain. In *Proc. of the 1997 American Control Conference*, volume 1, pages 636–640, 1997.
- [17] M. Filippa, C. Mi, J. Shen, and C. Stevenson. Modeling of a hybrid electric vehicle powertrain test cell using bond graphs. *IEEE Transactions on Vehicular Technology*, 54(3):837–845, 2005.